Elongational Flow Studies on the Molecular Properties of Collagen and Its Thermal Denaturation

NAOKI SASAKI*, EDWARD D. T. ATKINS, and W. STEPHEN FULTON†

H. H. Wills Physics Laboratory, University of Bristol, Tyndall Avenue, Bristol BS8 1TL, United Kingdom

SYNOPSIS

An elongational flow method established in polymer physics was applied to study dynamic structure and properties of biopolymers in solution. Type I collagen solutions in the dilute to semidilute region are studied in elongational flow fields, generated in a Taylor four-roll mill, for temperatures from 20°C through the melting temperature to 60°C. A nonlocalized birefringent signal, characteristic of stiff molecules, is observed at all temperatures. The conformational changes as a function of temperature can be divided into two separate temperature dependent stages. In stage I, at lower temperatures, the collagen molecule behaves as a rigid rod and the birefringent signal Δn rises as a function of increasing strain rate $\dot{\epsilon}$. Throughout this stage the type of molecular interaction in semidilute solution does not change but the rate of interaction is increased by thermal excitation. In stage II, a characteristic criticality in the Δn vs. $\dot{\epsilon}$ plot is observed. For strain rates up to a characteristic value, $\dot{\epsilon}_0$, the birefringence remains zero and for $\dot{\epsilon} > \dot{\epsilon}_0$ whole field bright birefringence is observed. The plateau values of birefringence, Δn_p, at high strain rates in the Δn vs. $\dot{\epsilon}$ curve decreased with rising temperature in stage II. This criticality in behavior and the decreasing tendency in Δn_p with temperature are explained by the collagen molecule changing to a hinged-rod conformation. Thus the untwining of collagen as a function of temperature initiates at several places simultaneously, probably at specific amino acid sequences, within the collagen rodlike molecule.

INTRODUCTION

Investigations on the response of polymer molecules to pure elongational flow provide valuable information on the molecular process of chain extension, relaxation, and orientation of molecules and is an important part of polymer physics. Previous studies in this laboratory have examined the response of flexible[1-3], semiflexible,[4] and rigid-rod-like[5,6] polymer molecules in well-defined elongational flow fields. In the course of these investigations, methods have been developed in which elongational flow fields can be created and the resulting orientation, stretching, and relaxation monitored by measurement of mangitude and character of the birefringent signal.[7]

The elongational flow method can distinguish between flexible polymer chains and rigid-rod-like chains. For flexible molecules, flow-induced birefringence is localized along the symmetry axis for opposed jets, or along the exit symmetry plane in the cross-slots or four-roll mill.[7] In a birefringence (Δn) vs. strain rate ($\dot{\epsilon}$) plot, at small $\dot{\epsilon}$'s, Δn remains zero and then increases rapidly at a critical strain rate $\dot{\epsilon}_c$, as shown diagrammatically in Figure 1 (a). The phenomenon has been predicted theoretically as the coil–stretch transition of a polymer chain.[8] Measurement of $\dot{\epsilon}_c$ enables the conformational relaxation time τ of a random coil to be obtained[8] using the relation

$$\tau \sim 1/\dot{\epsilon}_c \qquad (1)$$

In the case of rigid-rod-like molecules, nonlocalized

* To whom correspondence should be addressed at Department of Applied Materials Science, Muroran Institute of Technology, 27-1 Mizumoto, Muroran 050, Japan.

† Present address: The Malaysian Rubber Producers' Research Association, Tun Abduk Razak Laboratory, Brickendonbury, Hertford, SG13 8NL, U.K.

Journal of Applied Polymer Science, Vol. 42, 2975-2985 (1991)
 CCC 0021-8995/91/112975-11$04.00

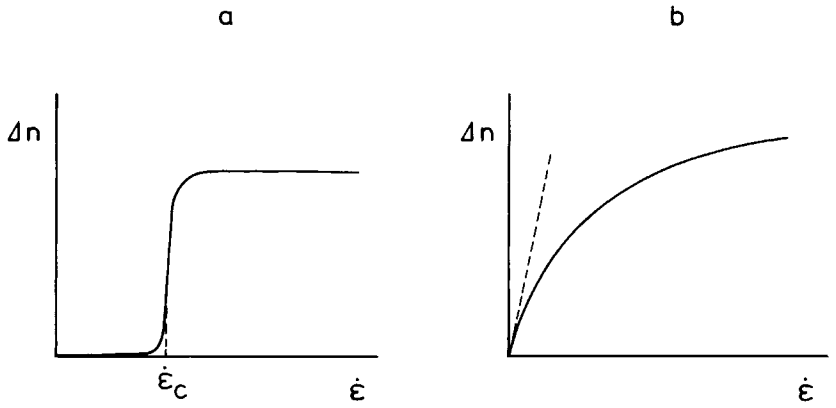

Figure 1 Schematic diagrams of elongational flow-induced birefringence Δn vs. strain rate $\dot{\epsilon}$ for (a) flexible molecules and (b) rigid-rod-like molecules.

birefringence is observed over the whole irradiated field.[5,6] Δn increases continuously with $\dot{\epsilon}$, as shown in Figure 1 (b). From the initial gradient of Δn vs. $\dot{\epsilon}$ plot, the rotational diffusion coefficient in an isotropic environment, D_r, is obtained by the relation[3,9]

$$D_r = 2\dot{\epsilon}/15(\Delta n/\Delta n_o) \quad (2)$$

where Δn_o is the birefringence from a completely oriented polymer solution.

It is known that biopolymers such as collagen, DNA, and the α-helical poly(α-amino acids) give a helix–coil transition under certain environmental changes such as temperature, pH, ionic strength, and so on. In the transition process, the molecular conformation changes from a rigid-rod-like to flexible coil. There have been several models proposed for the conformational changes on the basis of thermodynamic consideration for this transition. Using elongational flow, it is interesting to observe the helix–coil transition of biopolymers as well as their rod or flexible coil states. The aim of this work is to pursue the possibility of the elongational flow field as a new method for investigating dynamic structures and properties of biopolymers in solution.

We have studied the hydrodynamic process of helix–coil transition of type I collagen by using the elongational flow method. We have used the four-roll mill apparatus since only relatively small quantities of sample solution are needed and it is relatively straightforward to change the temperature of the system during the experiment.

In a solution of polymer molecules, the overall hydrodynamic behavior has been known to be affected largely by the length of the molecules and the magnitude and distribution of their molecular weight. In order to have a solution of monodisperse collagen molecules for this study, we have used collagen from lathyritic rats, which has no intermolecular covalent crosslinks.

EXPERIMENTAL

Materials

Type I collagen used in this study was prepared from tail tendon of lathyritic rats and kindly provided by Dr. V. Duance and Professor A. J. Bailey (AFRC Food Research Laboratory, Langford, Bristol, U.K.). Collagen was extracted from tissue by neutral salt (1 *M* NaCl in Tris-HCl buffer, pH 7.4 at 4°C). The suspension was centrifuged and the supernatant was dialized against 0.5 *M* acetic acid according to the procedure of Chandrakasan.[10] The acetic acid solution of collagen was purified further by centrifugation and dialysis. Finally the stock solution was prepared in 0.1 *M* acetic acid, pH 3.5 at collagen concentration of 2 mg/mL. The extracted collagen was characterized by SDS polyacrylamide gel electrophoresis. A minute portion of intramolecular crosslinks and the complete absence of any intermolecular crosslinks was found (V. Duance, unpublished result).

A sample solution was prepared by dissolving the stock solution into acidic glycerol, pH 3.5, in order to increase the viscosity of solution. Three sample solutions were prepared for temperature dependence measurements: 0.02% collagen and 89% glycerol solution, 0.008% collagen and 95% glycerol solution, and 0.002% collagen and 98% glycerol solution. A high concentration of glycerol was needed for the low collagen concentration sample for the sake of the accuracy of measurements at the initial part of Δn vs. $\dot{\epsilon}$ curve.

Apparatus

The four-roll mill system consists of four parallel and mutually counterrotating rollers positioned on the corners of a square and spinning on vertical axes. The system has been utilized by Taylor for the study of liquid droplets in the flow field and by Torza to investigate shear-induced crystallization.[11,12] The present experimental arrangements including an optical system for the observation has been described in detail elsewhere.[2,5,6] The apparatus was modified by constructing an electrically heated jacket to surround the solution and the temperature was measured and controlled with thermocouples. All the intensity measurements were made with polarizer and analyzer positioned at 45° relative to the mill inlet and outlet directions, respectively. In this optical arrangement, the birefringence Δn is well approximated by the square root of transmitted intensity provided that the retardation is small. Measurements of Δn as a function of $\dot{\epsilon}$ were made isothermally for the strain rate over the range from 0 to 240 s^{-1} and for the temperature ranging between 20 and 60°C. The increasing rate of the temperature between two successive measuring points was about 3°C/h. Because of the use of glycerol as a viscosity builder, we did not observe any evidence of turbulent flow in the system up to the maximum strain rate of 240 s^{-1}. It was found convenient to use an He–Ne laser and photodiode for intensity measurements and a tungsten lamp for visual observation.

RESULTS AND DISCUSSION

Visual Observations

At room temperature, when the polarizer and analyzer are positioned at 45° relative to the mill inlet and outlet direction, a uniformly bright field was observed within the area enclosed by the rollers. Dark streamlines were superimposed on the bright field. These are caused by density inhomogeneities along the stream lines in the system. With the polarizer and analyzer directions parallel and perpendicular to the entry and exit directions, the same area becomes uniformly dark. This means that the transmission axes of the birefringent solution coincide with these two directions. The effect of the elongational flow field generated by the four-roll mill is to produce a nonlocalized orientation of collagen molecule in the flow field.

The results suggest that collagen molecules at room temperature are rigid-rod-like. Rigid-rod-like molecules are known to orient parallel to the exit symmetry plane of the elongational flow field at the center of a four-roll mill.[5] In the case of collagen, it is not unreasonable to recognize that the rod axis of a molecule is oriented parallel to the exit symmetry plane within the center of the four-roll mill.

The same nonlocalized birefringence pattern was observed throughout the temperature-dependent experiments, up to the denaturation temperature of collagen. At higher temperatures though, the intensity was reduced and there was a zero–Δn region in the Δn vs. $\dot{\epsilon}$ plot before the increase of Δn with $\dot{\epsilon}$. At high temperatures, the collagen molecule is expected to be partly or almost completely untwined. There might be a possibility that part or all of the birefringence observed, at high temperatures in particular, originates from the untwined polypeptide chains extended by the flow field. In order to clarify the origin of the birefringence, measurement was made for a perfectly denatured sample at 60°C. A localized birefringence line is expected for flexible polymer chains but at no stage was this observed for the denatured sample. Thus any flexible coils formed would have a critical strain rate, $\dot{\epsilon}_c$, larger than the upper value of $\dot{\epsilon}$ generated by the apparatus used.

From these visual observations, it is concluded that the birefringence observed throughout the experiments originates from the orientation of rodlike molecules or the rodlike part of partly untwined collagen molecules.

Temperature Dependence of the Birefringence

As mentioned in the Experimental section, all the intensity measurements were made with polarizer and analyzer positioned at the 45° to the mill inlet and outlet directions, respectively.

Figure 2 shows the temperature dependence of Δn at $\dot{\epsilon} = 212\ s^{-1}$, Δn_{212}, for 0.02% (●), 0.008% (□) and 0.002% (○) collagen solutions. Up to certain temperature, Δn_{212} values are conserved at their room temperature values followed initially by a gradual and then finally a rapid decrease of Δn_{212} with temperature. In 0.002% solution, these features are not clear but the same character is observable. This temperature dependence of Δn_{212} corresponds to an untwining process of collagen molecule. The denaturation temperature of collagen is a function of the solvent and in our case the addition of glycerol is expected to raise the value above the 37°C for totally aqueous solutions.[13,14] In Figure 2, as discussed in the previous section, when Δn_{212} falls to zero, the system contains only random flexible coils. The temperature is approximately 55°C. It is not

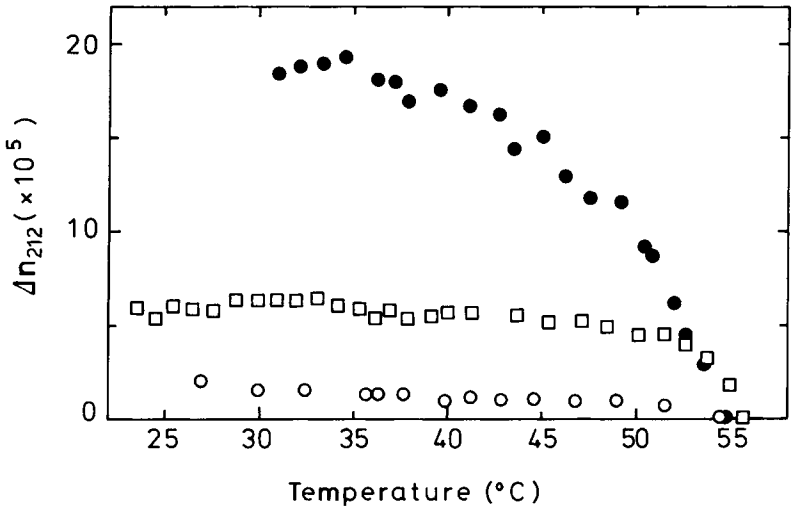

Figure 2 Temperature dependence of birefringence at the strain rate $\dot{\epsilon} = 212\ s^{-1}$, Δn_{212}, for concentrations of 0.02% (●), 0.008% (□), and 0.002% (○) of collagen solutions.

unreasonable to regard this temperature as a final temperature (T_f) of collagen denaturation in our system.

Figure 3 shows the Δn vs. $\dot{\epsilon}$ curves for 0.008% solution measured at 28.8, 43.7, and 53.8°C. In Δn vs. $\dot{\epsilon}$ curves at both 43.7 and 53.8°C, there are zero–Δn regions before the increase in Δn begins, whereas Δn increases with $\dot{\epsilon}$ at $\dot{\epsilon} = 0\ s^{-1}$ for the curve at 28.8°C. The temperature at which a Δn vs. $\dot{\epsilon}$ curve begins to have a zero–Δn region roughly corresponds to the temperature at the beginning of the gradual decrease of Δn_{212} with temperature. From these results we can divide the temperature dependence of Δn_{212} into two stages:

(1) *Stage I:* Δn_{212} values do not change with temperature and Δn increases with $\dot{\epsilon}$ from $\dot{\epsilon} = 0\ s^{-1}$ at each temperature.

(2) *Stage II:* Δn_{212} values decrease gradually and then rapidly with temperature and in the Δn vs. $\dot{\epsilon}$ plot there is a zero–Δn region before the increase in Δn with $\dot{\epsilon}$ begins. The beginning

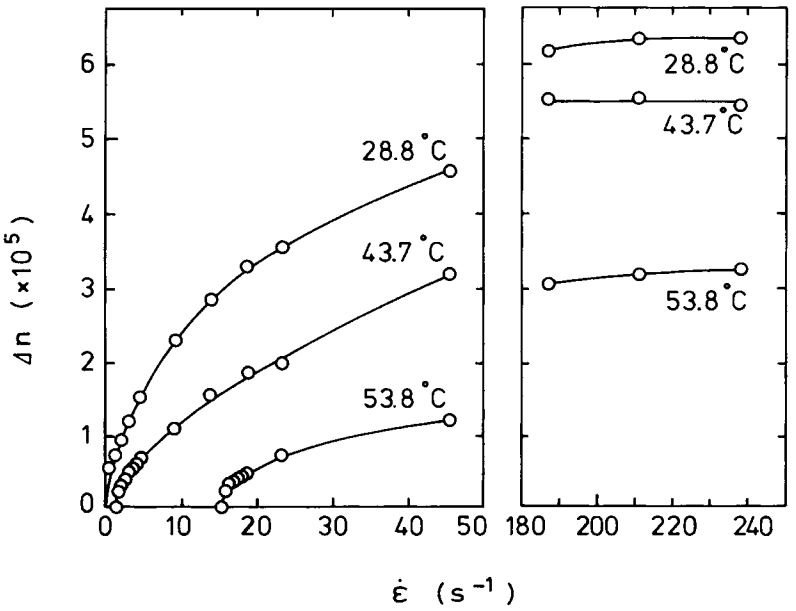

Figure 3 Elongational flow induced birefringence Δn plotted against strain rate $\dot{\epsilon}$ at indicated temperatures for 0.008% collagen solution.

temperature of this stage is considered to correspond to the beginning temperature of the denaturation of collagen.

Stage I ranges between room temperature and 38°C for 0.02% solution, 39°C for 0.008% solution, and 45°C for 0.002% solution. The difference in the terminal temperature for each concentration, for both stages, respectively, is expected to be caused by the difference in glycerol concentration in each solution. It changes the concentration and the state of water molecules around a collagen molecule, which has been known to affect the stability of a triple helix of collagen (in our case stabilize it).[13,14]

It appears that hydrodynamic properties of collagen molecule in each stage are different, and so each stage is discussed separately.

Stage I

In this stage, according to the classification of the elongational flow birefringence pattern, the collagen molecule seems to have the characteristics of a rigid-rod-like molecule. It has been known that the interaction among rigid-rod-like polymer molecules was classified according to the concentration of the solution of rodlike molecules, where the rodlike molecules were assumed to be monodisperse.[15] Let us suppose that the length of the molecule is L (nm) and the diameter is d (nm). When the number of polymers per unit volume, c, (nm^{-3}), is far smaller than L^{-3}, the solution is defined as dilute. In a dilute solution of rodlike polymer molecules, each molecule can rotate freely without any imposed restriction by other polymer molecules. When c increases far beyond L^{-3}, the dynamic properties of polymer solution drastically change because of the topological constraint that polymers cannot cross each other. The static properties do not change substantially if the concentration is smaller than $1/dL^2$. Polymer solution with concentration c in the range

$$L^{-3} \ll c \ll d^{-1}L^{-2} \qquad (3)$$

are defined as semidilute. In our case, solutions of 0.008 and 0.02% are classified semidilute and 0.002% is dilute by the above criteria.

We have determined the rotational diffusion coefficient D_r of rigid-rod-like collagen molecules from the initial slope of Δn vs. $\dot{\epsilon}$ curve using eq. (2). Figure 4 shows the temperature dependence of D_r for 0.002% solution. The solid line represents the temperature dependence of D_r for a rigid rod of the size of a collagen molecule in glycerol solution, using the

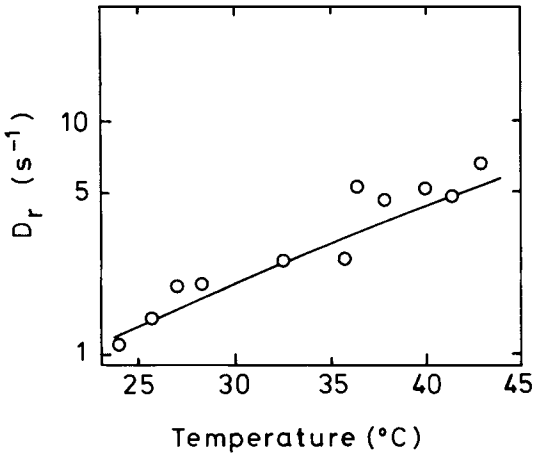

Figure 4 Temperature dependence of the rotational diffusion coefficient D_r for 0.002% collagen solution. The solid curve represents the temperature dependence of D_r of a rigid rod of the size of a collagen molecule using the Broersma equation for the rigid rod.

Broersma equation for rigid rods.[16,17] Experimental points agree well with the theoretical curve. This coincidence between experimental data and theoretical values for rotational diffusion coefficient in dilute solution indicates that collagen molecule is well modelled by a rigid rod. On the other hand, D_r in semidilute solutions is smaller than their theoretical values, D_{r0}, as shown in Figures 5(a) and (b). In both cases, D_r/D_{r0} values do not look to change through the temperature range. $D_r/D_{r0} < 1$ might be explained by assuming that in 0.008 and 0.02% collagen solutions, molecules would be semiflexible.[18] It is, however, difficult to consider (1) that the hydrodynamic properties would be changed from rigid to semiflexible only by increasing the concentration from dilute to semidilute and (2) that the flexibility, D_r/D_{r0} value according to Hagerman and Zimm,[18] does not change with temperature. We believe it more reasonable to assume that the rigid rod model is still suitable for collagen molecules in these concentrations. The Doi–Edwards theory explains $D_r/D_{r0} < 1$ by the interaction of rigid rod molecules: The circumstance about a molecule in the solution was simplified as one rod under consideration and its surrounding cage made by the surrounding rod like molecules; the rheological properties of the system was considered to be governed by the escaping process of the molecules from the cage.[15] The fact that, through the temperature range corresponding to stage I, the value of D_r/D_{r0} does not change means that in this stage the type of molecular interaction, i.e., the surrounding cage and

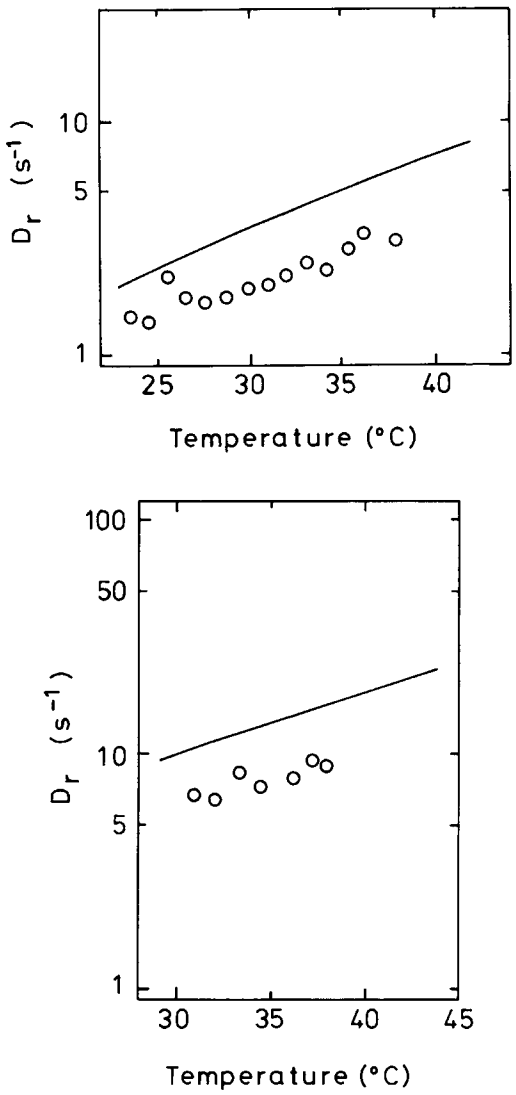

Figure 5 Temperature dependence of D_r for (a) 0.008% and (b) 0.02% collagen solutions. The solid curve in each figure represents the temperature dependence of D_r of the rigid rod estimated by the Broersma equation.

the escaping process of the molecule in problem from the cage, does not change.

A diffusion coefficient in semidilute solution, D_r, has been theoretically estimated as[19,20]

$$D_r = D_{r0}\beta(cL^3)^{-2} \qquad (4)$$

where β is an adjusting parameter originally expected to be of the order of unity. Many experimental results, however, show that the value of β falls in the range between 10^2 and 10^6.[21-25] In Figure 6, logarithmic value of D_r/D_{r0} are plotted against log (cL^3). The three dashed lines (a), (b), and (c) represent the c^{-2} relation [eq.(4)] for $\beta = 10^4$ (cowhide, shortened collagen), 3×10^6 (rat tail tendon), and 6×10^6 (cowhide), respectively.[24,25] It is not clear if these β values not for monodisperse collagen solution[24,25] are immediately applicable to our monodisperse system. According to these three dashed lines, however, we can imagine the shape of the concentration dependence of D_r/D_{r0} curve in our case: Our semidilute resultant values of D_r/D_{r0} do not obey eq. (4) provided that $\beta \sim 1$, but if we can assume $\beta \gg 1$, as the three dashed lines in Figure 6, our values can be considered to be placed at the intermediate region between plateau and c^{-2} regions in the D_r/D_{r0} vs. c curve.

In the Doi–Edwards theory, the steady state solutions for the orientational distribution function includes only one dimensionless parameter, $\dot{\epsilon}/D_r$ and consequently any average over the distribution function depends on $\dot{\epsilon}$ in the combination of $\dot{\epsilon}/D_r$.[20] This suggests that if the strain rate is normalized by the rotational diffusion coefficient, the elongational flow data for each concentration and temperature will fall on a universal master curve:

$$\Delta n = cAf(\dot{\epsilon}/D_r). \qquad (5)$$

Here f is the function of the valuable $\dot{\epsilon}/D_r$ and depends on parameters such as a specific molecular weight distribution and a molecular interacting mode. c is the concentration (in %) and A is a proportionality constant associated with the intrinsic optical anisotropy of the system. Figures 7(a) and

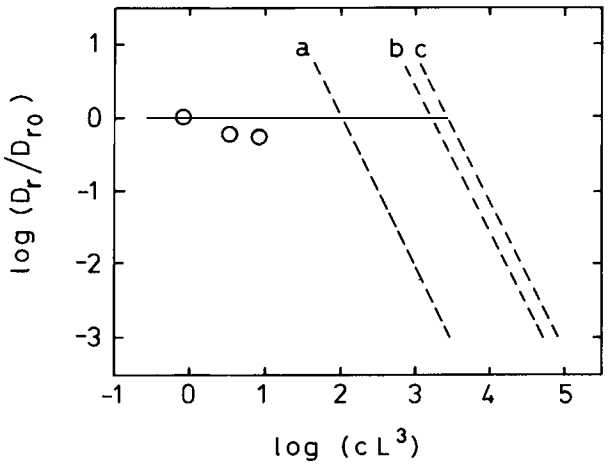

Figure 6 Logarithmic values of D_r/D_{r0} plotted against the normalized concentration (cL^3). The solid horizontal line represents the relation $D_r/D_{r0} = 1$. The dashed lines (a), (b), and (c) represent the c^{-2} relation for $\beta = 10^4$ (cowhide, shortened collagen), 3×10^6 (rat tail tendon) and 6×10^6 (cowhide) respectively.[24,25]

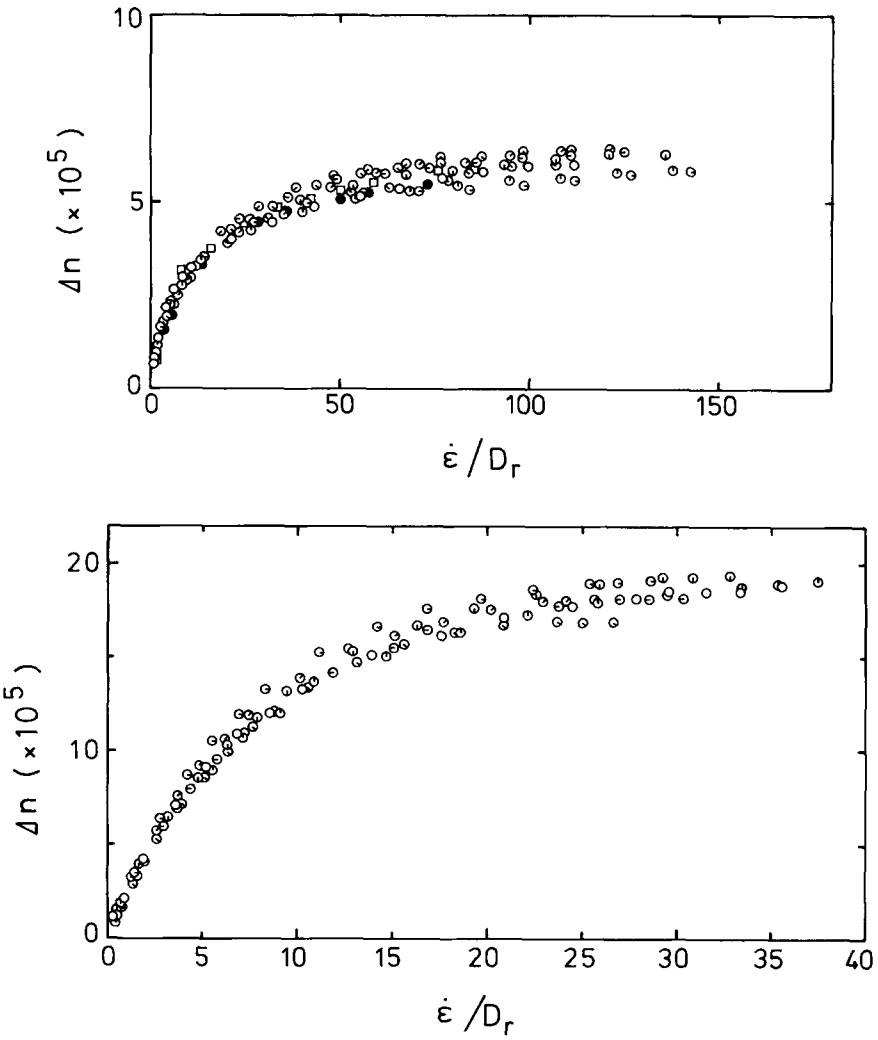

Figure 7 Δn plotted against the normalized strain rate $\dot{\epsilon}/D_r$ for 0.008% solution. (a) for temperatures 25.5°C (○), 26.5°C (Ⓘ), 27.6°C (⊖), 28.8°C (Ⓘ), 30.0°C (⊖), 31.0°C (⊘), 32.0°C (⊘), 33.1°C (⊘), 34.2°C (⊘), 35.4°C (□), and 36.2°C (●); and for 0.02% solution (b) for temperatures 31.0°C (○), 32.1°C (Ⓘ), 33.3°C (⊖), 34.5°C (Ⓘ), 36.2°C (⊖), 37.2°C (⊘), and 37.9°C (⊘).

(b) show the Δn plotted against the normalized strain rate $\dot{\epsilon}/D_r$ for 0.008 and 0.02% solutions, respectively, at temperatures in the stage I. In Figure 8, Δn scaled by c is plotted against the normalized strain rate for 0.02 and 0.008%, where $\dot{\epsilon}/D_r$ for the data of 0.02% solution is modified by the factor $D_{r0}(0.02)/D_{r0}(0.008)$ at each temperature. These scaling procedures indicate that throughout stage I, as the function f itself is unchanged, in semidilute solution the type of molecular interaction does not change but the rate of the interaction processes is increased by thermal excitation.

In this study, we found that collagen molecules in the stage I region can be well modelled as rigid rods. The conclusion was deduced from the following facts: (1) Elongational flow birefringence pattern was that of rigid-rod-like molecules, (2) the coincidence of experimental D_r values for dilute solution with those of theoretical ones for rigid rod, and (3) molecular interaction in semidilute solution was well explained by the theoretical expression for rigid rod. The discussion on the basis of these facts were solid enough to decide that molecules in solution were rigid-rod-like. This conclusion is in agreement with early collagen studies in which the type I collagen molecule in solution has generally been assumed to be a rigid rod.[26,27] Later results from hydrodynamic and morphological investigation of collagen mole-

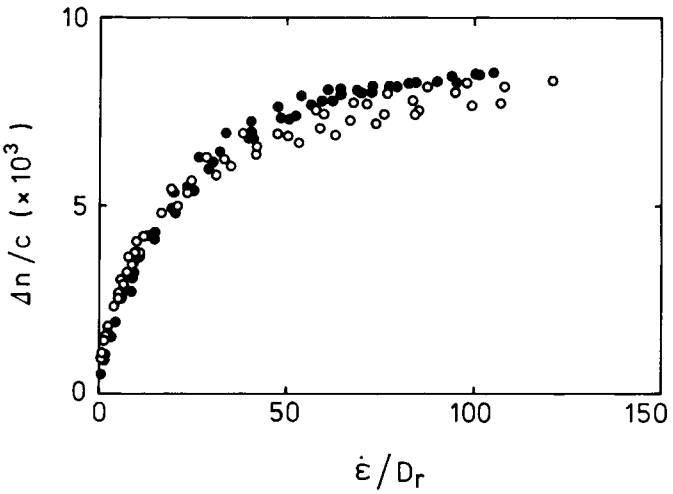

Figure 8 $\Delta n/c$ plotted against $\dot{\epsilon}/D_r$ for 0.02% (●) and 0.008% (○) collagen solution. The $\dot{\epsilon}/D_r$ value for 0.02% solution data was modified by the factor $D_{r0}(0.02)/D_{r0}(0.008)$.

cules, however, have suggested that the collagen molecule behaves as a semiflexible rod, although there have been some inconsistencies in detail.[28-31]

This discrepancy is considered to be related to the difficulty of determining the degree of flexibility or rigidity of the molecule by our method as it is not in a complete form now. Young's moduli of collagen and DNA are reported to be 4 and 0.1 GPa, respectively.[31] Preliminary elongational flow experiments on lambda-phage DNA show that the DNA molecule is semiflexible. Thus the critical stiffness beyond which the elongational flow method indicates that the molecule is rigid-rod-like would exist between the values of 4 and 0.1 GPa.

It is of necessity to obtain the knowledge about the critical stiffness of a molecule and to establish a quantitative way of determining molecular parameters in solution. Such an investigation is now in progress in this laboratory.

Stage II

The characteristic manifested by collagen solution in this stage is that in the Δn vs. $\dot{\epsilon}$ plot, there is a zero-Δn region before the increase in Δn with $\dot{\epsilon}$ begins, which is contrasted with the Δn-$\dot{\epsilon}$ pattern in stage I. Also the observed birefringence at $\dot{\epsilon}$ of 100 s^{-1} was not localized, which is contrasted with the case of flexible polymer chains. Figure 9 shows the temperature dependence of the characteristic strain rate $\dot{\epsilon}_0$, at which Δn begins to increase from zero, for temperatures corresponding to Stage II for 0.008% solution. At low temperatures within this stage, the absolute value of plateau birefringence in Δn vs. $\dot{\epsilon}$ curve, Δn_p ($\simeq \Delta n_{212}$ in Fig. 2), decreases gradually with temperature while the $\dot{\epsilon}_0$ value is almost constant. Near the terminal temperature of the helix-coil transition of collagen, the Δn_p value rapidly decreases and the $\dot{\epsilon}_0$ value rapidly increases.

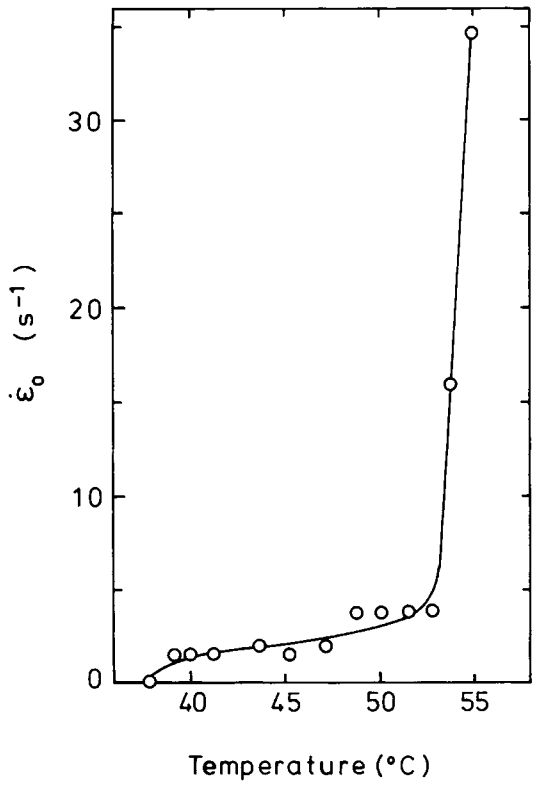

Figure 9 The characteristic strain rate $\dot{\epsilon}_0$ plotted against temperature for 0.008% collagen solutions.

From the results of the experiment on the denaturated sample (as in the Visual Observation section), it is noted that the $\dot{\epsilon}_0$ observed are not related to the coil–stretch transition. Although not shown, the $\dot{\epsilon}_0$ was also found for the 0.002% dilute solution. The whole field nonlocalized birefringence pattern begins at $\dot{\epsilon} = 0\ s^{-1}$, when the temperature of 0.008% solution at 40°C (in stage II) was reduced to 33 and 28°C (stage I). These two results suggest that the existence of $\dot{\epsilon}_0$ with nonlocalized birefringence is attributable, not to a molecular entanglement which has been expected for some flexible polymers in semidilute solution,[32] but to a change in each molecule, in particular a change in molecular conformation. Thus we believe the changes we observe are related directly to the untwining process of the collagen molecules.

There have been several models of helix–coil transition for multistranded biopolymers including collagen. Each of them has assumed the conformation of the molecule during the transition. Traditionally suggested conformational changes in the helix–coil transition are as follows (Fig. 10):

(1) All-and-None Model: The system is a mixture of perfectly untwined coils and complete rigid rods. With the increase in temperature the population of untwined molecules will increase. Such a system is the basis of an all-or-none type transition model.[33]

(2) Dumbbell Model: Molecular untwining occurs at both ends of a molecule. So a partly untwined molecule would behave as a dumbbell. Such a conformation is assumed as the basis of unzippering models of helix–coil transitions for multistranded biopolymers including collagen.[34,35]

(3) Hinged Rod Model: Molecular untwining occurs at certain sites on molecular rod, not only at both ends. Each untwined part would have a role of hinge between broken shorter rods. In the case of collagen, the model was assumed on the basis of the fact that the presence of pyrrolidine ring-containing residues in collagen interrupts the formation of hydrogen bonds and thus affects the melting behavior.[36,37]

Models (1) and (2) will be expected to show a Δn vs. $\dot{\epsilon}$ pattern similar to that for a rigid rod {whole field brightness begins at $\dot{\epsilon} = 0\ s^{-1}$ [Fig. 1(b)]} in the stage II temperature range, because, for (1), rigid rods always remain and they will produce a Δn signal at every value of $\dot{\epsilon}$ and, for (2), the dumbbell-like molecules will behave essentially as a rigid rod. These expectations are contrary to our observations and experimental results.

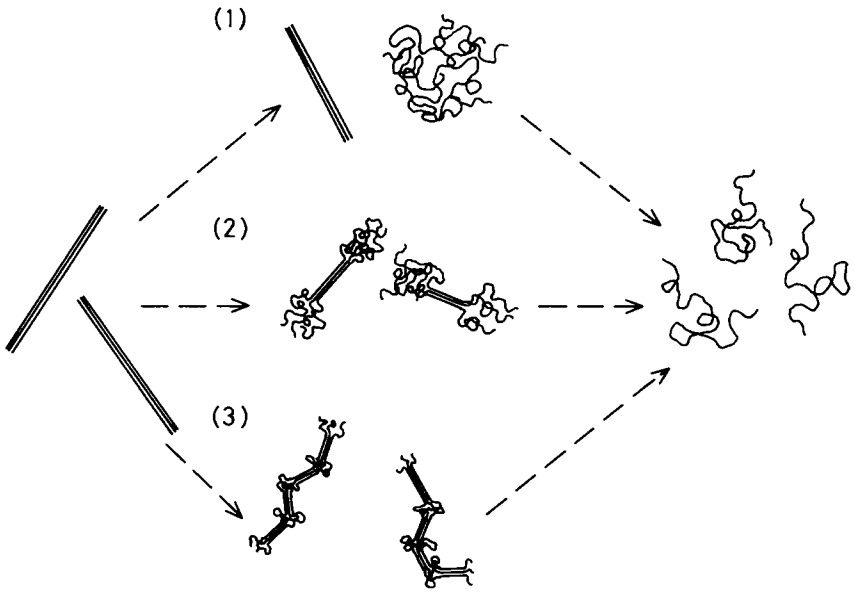

Figure 10 Traditionally suggested conformational changes during the helix–coil transition of collagen: (1) all-and-none model; (2) dumbbell model; (3) hinged rod model. In practice, the short rigid segments would orient more randomly than that depicted in the diagram.

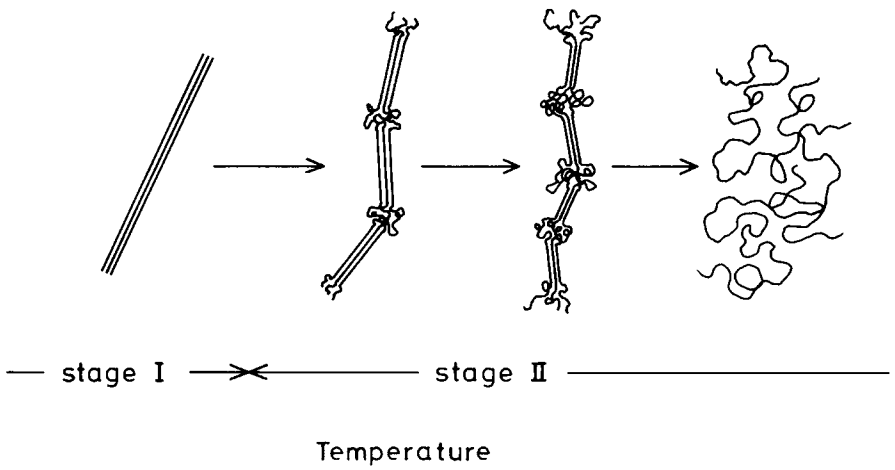

Figure 11 Schematic representation of collagen denaturation by temperature. In practice, the short rigid segments would orient more randomly than that depicted in the diagram.

The appearance of nonlocalized birefringence at $\dot{\epsilon}_0$ will be realized if a molecule has a conformation modeled as a freely jointed or hinged rod as in model (3). According to this model, a collagen molecule starts to flex at several places simultaneously within the rod. The collagen is regarded as a hinged rod with several hinges. An outlined shape of a molecule should be a stumpy spheroid as a result of entropic forces between segmantal shortened rods. In a spheroid, short rods are oriented randomly. At small $\dot{\epsilon}$, the spheroids will respond to the elongational flow field so as to have their longer axis parallel to the exit symmetry plane of four-roll mill; but the short rods will remain oriented at random, so that there should be no birefringent signal. The appearance of nonlocalized birefringence will occur at the strain rate $\dot{\epsilon}_0$ at which the enlongational force overcomes the entropic forces in a molecule in the flow field. As a result, for $\dot{\epsilon} < \dot{\epsilon}_0$, we have a zero–$\Delta n$ region, and for $\dot{\epsilon} > \dot{\epsilon}_0$ we have a whole field brightness which begins at $\dot{\epsilon} = \dot{\epsilon}_0$.

Figure 11 shows schematically the model (3) applied to the collagen. We can consider a suitable explanation of the phenomenon occurring in stage II on the basis of the process shown in this Figure 11. The intrinsic tendency of collagen to have hinges inside a rigid-rod-like molecule has been pointed out.[38] In stage II, initially the Δn_p value is almost unchanged with temperature as compared with the value in stage I. So at lower temperatures in stage II the molecule is generally a rod but a small amount of untwined part which behaves as hinges. Such a hinged rod is considered to recover its initial rigid rod conformation straightforwardly on reducing the temperature to that of stage I. Preliminary experiments were made for 0.008% collagen and 98% glycerol solution to confirm this behavior. In the Δn–$\dot{\epsilon}$ pattern at 40°C (stage II), there was a zero–Δn region. At 33 and 28°C (stage I) reduced from 40°C there was no evidence of $\dot{\epsilon}_0$ at all. It was also noticed that within experimental error the value of Δn_p recovers to its initial value at room temperature when the temperature was reduced to 33 and 28°C.

By the $\dot{\epsilon}_0$ values and the temperature dependence of Δn_p, the untwining process must be expected as follows. With the increase in temperature, the number of the hinges of the same size gradually increases. Near the helix–coil transition temperature of collagen, the number and the size of the hinges would rapidly increase by untwining parts interreconnecting one another. Above the transition temperature, there are only flexible random coils left.

The elongational flow studies have, thus, revealed the dynamic structure of collagen molecule during helix–coil transition to be hinged-rod-like on the basis of traditional models for conformation of collagen during helix–coil transition. We believe that the elongational flow method is thus proven to be useful to study dynamic structures and properties of biopolymers in solution.

We wish to acknowledge the support of Venture Research Unit of British Petroleum International. The authors also thank Dr. V. Duance and Professor A. J. Bailey of AFRC Institute of Food Research, Bristol Laboratory, for kindly supplying samples; Dr. J. L. Gathercol for helpful suggestions about the sample preparation; Dr. J. A. Odell and Professor A. Keller for their stimulating discussions throughout this work.

REFERENCES

1. M. R. Mackley and A. Keller, *Phil. Trans. Roy. Soc. (London)*, **A278** 29–66 (1975).
2. D. G. Crowley, F. C. Frank, M. R. Mackley, and R. G. Stephenson, *J. Polym. Sci. Polym. Phys. Ed.*, **14,** 1111–1119 (1976).
3. D. P. Pope and A. Keller, *Colloid Polym. Sci.*, **255,** 633–643 (1977).
4. M. J. Miles, K. Tanaka, and A. Keller, *Polymer*, **24,** 1081–1088 (1983).
5. J. A. Odell, A. Keller, and E. D. T. Atkins, *Macromolecules*, **18,** 1443–1453 (1985).
6. J. A. Odell, E. D. T. Atkins, and A. Keller, *J. Polym. Sci. Polym. Lett. Ed.*, **21,** 289–300 (1983).
7. A. Keller and J. A. Odell, *Colloid Polym. Sci.*, **263,** 181–201 (1985).
8. P. G. De Gennes, *J. Chem. Phys.*, **60**(2), 5030–5042 (1974).
9. A. Peterlin, *J. Phys. Chem.*, **84,** 1650–1657 (1980).
10. G. Chandrakasan, K. A. Torkia, and K. A. Piez, *J. Biol. Chem.*, **251,** 6062–6067 (1976).
11. G. I. Taylor, *Proc. Roy. Soc. (London)*, **146,** 501–523 (1934).
12. S. J. Torza, *J. Polym. Sci. Polym. Phys. Ed.*, **13,** 43–57 (1975).
13. P. J. Flory and R. R. Garret, *J. Am. Chem. Soc.*, **80,** 4836–4845 (1958).
14 D. Herbage, A. Harris, and G. Vallet, *Biochem. Biophys. Acta*, **168,** 544–554 (1968).
15. M. Doi and S. F. Edwards, *The Theory of Polymer Dynamics*, Clarendon, Oxford, 1986
16. S. Broersma, *J. Chem. Phys.*, **32,** 1626–1631 (1960).
17. J. B. Segur and H. E. Oberstar, *Ind. Eng. Chem.*, **43**(9), 2117–2120 (1951).
18. P. J. Hagerman and B. H. Zimm, *Biopolymers*, **20,** 1481–1502 (1981).
19. M. Doi and S. F. Edwards, *J. Chem. Soc. Faraday Trans. 2*, **74,** 560–570 (1978).
20. M. Doi and S. F. Edwards, *J. Chem. Soc. Faraday Trans. 2*, **74,** 981–932 (1978).
21. J. F. Maguire, J. P. McTague, and F. Rondelez, *Phys. Rev. Lett.*, **45,** 1891–1894 (1980).
22. Y. Mori, N. Ookubo, R. Hayakawa, and Y. Wada, *J. Polym. Sci. Polym. Phys. Ed.*, **20,** 2111–2124 (1982).
23. I. Teraoka, N. Ookubo, and R. Hayakawa, *Phys. Rev. Lett.*, **55**(24), 2712–2715 (1985).
24. A. W. Chow, G. G. Fuller, and J. A. Madri, *Macromolecules*, **18,** 793–804 (1985).
25. A. W. Chow, G. G. Fuller, D. G. Wallace, and J. A. Madri, *Macromolecules*, **18,** 805–810 (1985).
26. H. Boedtker and P. Doty, *J. Am. Chem. Soc.*, **78,** 4276–4280 (1956).
27. B. Obrink, *Eur. J. Biochem.*, **25,** 563–572 (1972).
28. H. Utiyama, K. Sakato, K. Ikehara, T. Setsuiye, and M. Kurata, *Biopolymers*, **12,** 53–64 (1973).
29. T. Saito, N. Iso, H. Mizuno, N. Onda, H. Yamato, and H. Odashima, *Biopolymers*, **21,** 715–728 (1982).
30. H. Hofman, T. Voss, K. Kuhn, and J. Engel, *J. Mol. Biol.*, **172,** 325–343 (1984).
31. H. F. Nestler, S. Hvidt, J. D. Ferry, and A. Veis, *Biopolymers*, **22,** 1747–1758 (1983).
32. J. A. Odell, A. Keller, and M. J. Miles, *Polymer*, **26,** 1219–1226 (1985).
33. N. Go and Y. Suezaki, *Biopolymers*, **12,** 1927–1930 (1973)
34. M. Schwarz, Jr. and D. Poland, *Biopolymers*, **13,** 687–701 (1974).
35. H. Wiedner, *Biopolymers*, **14,** 763–780 (1975).
36. J. P. Carver and E. R. Blout, in *Treatise on Collagen*, G. N. Ramachandran, Ed., Academic, London, Vol. 1, 1967, pp. 441–526.
37. F. R. Brown III, A. J. Hopfinger, and E. R. Blout, *J. Mol. Biol.*, **63,** 101–115 (1972).
38. E. J. Amis, C. J. Carriere, J. D. Ferry, and A. Veis, *Int. J. Biol. Macromol.*, **7,** 130–134 (1985).

Received September 27, 1990
Accepted October 5, 1990